European Journal of Pharmaceutics and Biopharmaceutics 74 (2010) 304–310

Contents lists available at ScienceDirect

European Journal of Pharmaceutics and Biopharmaceutics

journal homepage: www.elsevier.com/locate/ejpb

Research paper

Comparing different salt forms of rotigotine to improve transdermal iontophoretic delivery

O.W. Ackaert [a], J. Eikelenboom [a], H.M. Wolff [b], J.A. Bouwstra [a,*]

[a] Division of Drug Delivery Technology, Leiden/Amsterdam Center for Drug Research, Gorlaeus Laboratories, Leiden, The Netherlands
[b] UCB Schwarz Biosciences GmbH, Monheim, Germany

ARTICLE INFO

Article history:
Received 3 July 2009
Accepted in revised form 30 November 2009
Available online 5 December 2009

Keywords:
Solubility
Transdermal
Iontophoresis
Rotigotine
Salt form
Modeling

ABSTRACT

The transdermal delivery of a new salt form of the dopamine agonist rotigotine, rotigotine·H_3PO_4 is presented and compared to rotigotine·HCl. A comparison was made on the level of solubility, passive and iontophoretic delivery. Different aspects of the delivery were investigated: delivery efficiency, maximum flux, donor pH, electro-osmotic contribution and transport number. Changing the salt form from rotigotine·HCl to rotigotine·H_3PO_4 increases significantly the solubility and rules out the influence of NaCl on the solubility by the absence of the common-ion effect. At low donor concentration, no difference in transdermal delivery was observed between the salt forms. Due to an increase in the maximum solubility of rotigotine·H_3PO_4, a 170% increase in maximum flux, compared to rotigotine·HCl, was achieved. A balance between solubility and delivery efficiency can be obtained by choosing the correct donor pH between 5 and 6. A slight increase in electro-osmotic contribution and transport number was observed. Using the parameters, determined by modeling the *in vitro* transport, *in vivo* simulations revealed that with iontophoresis therapeutic levels can be achieved with a rapid onset time and be maintained in a controlled manner by adjusting the current density.

1. Introduction

Transdermal drug delivery is an attractive alternative for oral drug delivery and hypodermic injections. Different delivery methods have been investigated over the years to increase the drug delivery through the skin. One of the possibilities is iontophoresis. By applying a small current across the skin it is possible to enhance the transdermal delivery of small charged ionic molecules. One of the interesting properties of this technique is the possibility to modulate the transport rate into and through the skin. This is an important advantage for drugs with a narrow therapeutic window, such as dopamine agonists. Rotigotine is a dopamine agonist used for the symptomatic treatment of Parkinson's disease. Studies, investigating the transdermal iontophoretic delivery of rotigotine·HCl revealed that by applying an electrical current across the skin higher steady-state fluxes can be achieved with a shorter lag time compared to passive delivery. However, in these studies, the maximum solubility of rotigotine·HCl in the donor phase appeared to be the limiting factor for its iontophoretic transport through the skin [1–3]. Increasing the solubility of rotigotine can be achieved by changing the donor solution, e.g. by adding surfactants or co-solvents or changing the source of Cl^--ions. Another possibility to improve the solubility is altering the salt form of the drug of interest. In transdermal iontophoretic delivery, the chloride anion is often added to the donor phase at the anodal side to feed the electrochemical reaction. To increase the solubility of rotigotine, another counterion may be chosen to destabilize the crystal structure and therefore to increase the solubility of rotigotine in the buffer solution. In the current study, H_3PO_4 was chosen as an alternative salt form for rotigotine·H_3PO_4 accounts for 2% of the FDA approved NCE's in the period from 1995 to 2006, is biocompatible, has a low molecular weight and circumvents the common-ion effect in the donor phase, making it a very interesting candidate as salt form for iontophoresis [4]. Moreover, in the literature, very few reports investigating different salt forms for transdermal delivery were described. Fang et al. studied the passive and iontophoretic delivery of three different salts of the anion diclofenac, showing that the counter ion can affect the transdermal delivery [5,6].

In the current study, the solubility and transdermal delivery of rotigotine·H_3PO_4 were evaluated in comparison with rotigotine·HCl to illustrate the influence of the choice of a salt form on the passive and iontophoretic transport through the skin. In addition, the *in vitro* transport of rotigotine·H_3PO_4 was analyzed with compartmental modeling and the parameters were used to evaluate the iontophoretic delivery *in vivo* in a series of simulations.

* Corresponding author. Address: LACDR/DDT, Gorlaeus Laboratories, Einsteinweg 55, 2333 CC Leiden, The Netherlands. Tel.: +31 715274208; fax: +31 715274565.
E-mail addresses: bouwstra@lacdr.leidenuniv.nl, bouwstra@chem.leidenuniv.nl (J.A. Bouwstra).

0939-6411/$ - see front matter © 2009 Elsevier B.V. All rights reserved.
doi:10.1016/j.ejpb.2009.11.016

2. Materials and methods

2.1. Materials

Rotigotine·H_3PO_4 and rotigotine·HCl were kindly supplied by UCB Schwarz Biosciences GmbH (Monheim, Germany). Silver, silver chloride (purity > 99.99%), trypsin (Type III from bovine pancreas), trypsin inhibitor (Type II-S from soybean) and methanesulfonic acid were obtained from Sigma–Aldrich (Zwijndrecht, The Netherlands). Acetaminophen was purchased from Brocacef (Maarsen, The Netherlands) and D(−)-Mannitol was obtained from Scharlau Chemie SA (Barcelona, Spain). Spectra/Por® RC dialysis membrane sheets (cut-off value of 6000–8000 Da) were purchased from Spectrum laboratories, Inc. (Rancho Dominquez, CA, USA). Acetonitrile was purchased from Biosolve (Valkenswaard, the Netherlands). All other chemicals and solvents were of analytical grade. All solutions were prepared in Millipore water with a resistance of more than 18 MΩ cm.

2.2. Solubility of rotigotine·H_3PO_4

In order to compare the maximum solubility of rotigotine·H_3PO_4 with rotigotine·HCl, the solubility studies of rotigotine·H_3PO_4 were carried out as described by Nugroho et al. [3], who determined the solubility of rotigotine·HCl. Briefly, rotigotine·H_3PO_4 was solubilized in 10 mM citric buffer at pH 4, 5 and 6 with and without the presence of NaCl. Subsequent adjustment of pH in each test tube was performed by alternatingly adding small quantities of 1 M NaOH under continuous shaking and subsequent pH measurements, until the pH of each solution had stabilized at the original buffer value. Each solution was shaken for an additional 48 h, after which each solution was centrifuged and filtered. The concentration in each solution was determined by HPLC.

2.3. Capillary electrophoresis

The electrophoretic mobility of rotigotine·HCl and rotigotine·H_3PO_4 was investigated with capillary electrophoresis (CE). These experiments were performed according to a method described elsewhere [7]. Briefly, the electrophoretic mobility of the samples (0.5 mM) was determined in triplicate using a phosphate buffer pH 7.4 (Na_2HPO_4: 5.82 g l^{-1}; NaH_2PO_4: 5.1 g l^{-1}) as electrolyte solution (mobile phase).

2.4. Preparation of human stratum corneum

The preparation of human stratum corneum (HSC) was performed according to the method described previously [8]. Briefly, within 24 h after surgical removal of the human skin, residual subcutaneous fat was removed. Dermatomed human skin (DHS) was obtained by dermatoming the skin to a thickness of about 300 μm. In order to obtain HSC, DHS was incubated with the dermal side on Whatman paper soaked in a solution of 0.1% trypsin in 150 mM phosphate buffered saline (PBS) pH 7.4 (NaCl: 8 g L^{-1}, Na_2HPO_4: 2.86 g l^{-1}, KH_2PO4: 0.2 g l^{-1}, KCl: 0.19 g l^{-1}) overnight at 4 °C and subsequently for 1 h at 37 °C after which HSC was peeled off from the underlying viable epidermis and dermis. HSC was subsequently washed in a 0.1% trypsin inhibitor solution in Millipore water and several times in water and stored in a desiccator in a N_2 environment.

2.5. In vitro transport studies

A 9-channel computer-controlled power supply was used to provide a constant direct current (Electronics Department, Gorlaeus Laboratories, Leiden University, The Netherlands) during iontophoresis. The system was equipped with differential input channels per current source enabling online measurement of the electric resistance across HSC in each diffusion cell. Ag/AgCl was used as driver electrode pair. All transport experiments were carried out using a three chamber continuous flow through cell as described elsewhere [8]. The donor formulation, buffered with a 10 mM citric buffer, was applied at the anodal side. The cathodal chamber was filled with PBS pH 7.4. The acceptor phase, maintained at 32 °C, was continuously perfused with PBS pH 6.2 (NaCl: 8 g l^{-1}, KCl: 0.19 g l^{-1}, $Na_2HPO_4{\cdot}2H_2O$: 0.43 g l^{-1}, KH_2PO_4: 0.97 g l^{-1}) at a flow rate of 7.0 ml h^{-1}. Unless described elsewhere, the following protocol for the iontophoresis experiments was used: 6 h of passive diffusion, followed by 9 h of iontophoresis with a current density of 500 μA cm^{-2} and 5 h of passive diffusion. Samples were collected every hour with an automatic fraction collector (ISCO Retriever IV, Beun De Ronde BV, Abcoude, The Netherlands). The specific conditions of the individual transport studies are described below.

2.5.1. Flux of rotigotine·H_3PO_4 vs. rotigotine·HCl

The donor concentration of rotigotine·H_3PO_4 and rotigotine·HCl was kept constant (3.7 mM). The donor phase was buffered at pH 5 and contained 68 mM NaCl.

2.5.2. $Flux_{ss}$ vs. donor concentration rotigotine·H_3PO_4 and influence of pH

In these transport studies, four different concentrations rotigotine·H_3PO_4 (4.4 mM, 9.5 mM, 22.2 mM and 47.5 mM), buffered at pH 5, were used. Thereby, the transport of rotigotine·H_3PO_4 (4.4 and 13.0 mM), buffered at pH 6 was investigated as well. All transport experiments were performed in the presence of 68 mM NaCl in the donor phase.

2.5.3. Electro-osmotic flow

The donor concentration of rotigotine·H_3PO_4 was 3.9 mM and 11.6 mM. Acetaminophen (15 mM) was added to the donor phase as a marker for the electro-osmotic flow. The donor phase was buffered at pH 5 and contained 68 mM NaCl.

2.5.4. Current density flux-relationship

The relationship between the current density was studied with a rotigotine·H_3PO_4 concentration of 31.3 mM, buffered with a citric buffer at pH 5.5, containing 68 mM NaCl. The following protocol was used: 6 h passive + 6 h 166 μA cm^{-2} + 6 h 333 μA cm^{-2} + 6 h 500 μA cm^{-2} + 6 h passive.

2.6. Analytical method

Prior to and at the end of a transport study, the pH of donor and acceptor compartment was measured. All samples of the iontophoretic transport studies were analyzed by RP-HPLC using a Superspher® 60 RP-select B, 75 mm × 4 mm column (Merck KGaA, Darmstadt, Germany). Rotigotine was detected using a scanning fluorescence detector (Waters™ 474, Millipore, Milford, MA, USA) at excitation and emission wavelengths of 276 and 302 nm. Acetaminophen was detected using a UV detector (Dual λ Absorbance Detector 2487, Waters, Milford, USA) at a wavelength of 254 nm. Filtered and degassed mobile phase contained 60% H_2O (v/v), 40% ACN (v/v) and 0.05% methanesulfonic acid (v/v). The injection volume was 50 μL and the flow rate was set to 1.0 mL min^{-1}.

The concentration of rotigotine was quantified according to three standards with a concentration of 0.005, 2 and 5 μg mL^{-1}. The intra-assay variation of the retention time and of the area was less then 2.0%. For acetaminophen, calibration curves showed a linear response when using concentrations of compounds between 0.1 and 40 μg mL^{-1} (R^2 > 0.9999). The limit of detection

(LOD) and limit of quantification (LOQ) of acetaminophen were experimentally determined at 5.8 and 9.6 ng mL^{-1}, respectively. According to the literature, the limit of detection of rotigotine (base) was 11 ng mL^{-1} [2].

2.7. Determination of the passive, electro-osmotic and electromigrative flux

The total iontophoretic flux consists of the passive flux (J_{pass}), the electro-osmotic flux (J_{EO}) and the electromigrative flux (J_{EM}). The passive flux is calculated during 6 h prior to the iontophoretic phase. The neutral permeant acetaminophen was added to the donor solution as a marker molecule for quantification of the electro-osmotic flow during iontophoretic transport. The electromigrative flux is calculated by subtracting the passive and electro-osmotic flux from the total flux.

2.8. Data analysis

To calculate the steady-state flux during passive and iontophoretic transport, the cumulative flux of the transport was plotted as a function of time. The steady-state flux was estimated from the linear part of the slope of this plot according to the permeation lag-time method [8]. All data are presented as mean ± standard deviation (SD). When a statistical analysis was performed comparing only two groups, a Student's *t*-test was used. When three or more groups were compared, a one-way ANOVA statistical analysis was executed. If the overall *p*-value was less than 0.05, a Bonferronni post-test was applied to compare different groups. For all statistical analysis, a significance level of $p < 0.05$ was used.

2.9. In vitro modeling and in vivo simulation

Next to the permeation lag-time method, the data of the *in vitro* transport of rotigotine·H_3PO_4 at the selected condition (donor pH 5, donor conc 47 mM) was analyzed using nonlinear mixed effects modeling with the compartmental models described elsewhere [9]. Briefly, in these models, the starting point was a zero-order mass transport from the donor solution into the skin during and after iontophoresis. The equations, to describe *in vitro* iontophoretic transport during current application:

$$J(t) = \frac{I_0}{S}(1 - e^{-K_R\cdot(t-t_L)}) \quad (1)$$

$$J_{ss} = \frac{I_0}{S} \quad (2)$$

$$J(t) = \frac{P_{PI}}{S}(1 - e^{-K_R\cdot(t-t_L)}) + \frac{I_0}{S}(1 - e^{-K_R\cdot(T-t_L)})\cdot e^{-K_R(t-T)} \quad (3)$$

where $J(t)$ is the flux at time t and S is the diffusion area, K_R is a first-order skin release rate constant, I_0 the zero-order iontophoretic mass transfer from the donor compartment into the skin compartment during current application, t_L is the kinetic lag-time parameter, introduced to address the time required for drug molecules to enter the skin compartment, T is the time of current application and P_{PI} is the zero-order drug input due to the passive driving force in the post-iontophoretic period. Fitting the data was performed using the subroutines ADVANCE6 TRANS1 TOL = 5 from PREDPP in NONMEM (NONMEM version VI). Interindividual variability was modeled using an exponential error model and the residual error was characterized by an exponential and additive error model. The estimates of the population parameters were performed using a conventional first-order method. The model was evaluated graphically by plotting the population predicted vs. the observed flux and the individual predicted vs. the observed flux. Finally, from the final parameter estimates, a number of 100 samples were simulated. Post-processing of NONMEM simulations creating plots of visual predictive check (VPC) was done using Xpose 4, implemented in the software R (R version 2.7.0, R-foundation) [10].

The pharmacokinetic model used to simulate the iontophoretic delivery of rotigotine was based on a model described elsewhere [9]. Assuming a one-compartment model, different protocols were investigated for simulating the pharmacokinetic profile of iontophoretic delivery of rotigotine·H_3PO_4 during 24 h using a patch size of 10 cm^2:

Protocol 1: 24 h 350 μA cm^{-2}
Protocol 2: 5 h 350 μA cm^{-2} + 19 h 150 μA cm^{-2}

At time = 24 h, the patch was removed. In this case, the simulations were performed with the $SIMULATION function provided in NONMEM. A population of five subjects was simulated and the simulated population prediction was displayed graphically.

3. Results

3.1. Solubility and electrophoretic mobility of rotigotine·H_3PO_4

The results of the solubility assay of rotigotine·H_3PO_4 are presented in Table 1. At the selected pH values the addition of NaCl did not affect significantly the solubility of rotigotine·H_3PO_4 (2-way ANOVA; $p > 0.05$). This is in contrast with the results obtained with rotigotine·HCl by Nugroho et al. [3]. For rotigotine·HCl the solubility reduced tremendously after adding 68 mM NaCl. Furthermore decreasing the pH of the donor phase from 6 to 5 and again to pH 4 resulted in a significant increase in the solubility of rotigotine·H_3PO_4 (2-way ANOVA; $p < 0.05$).

The electrophoretic mobility of rotigotine·H_3PO_4 ($1.53 \pm 0.02 \times 10^{-4}$ cm^2 s^{-1} V^{-1}) showed no significant difference with the electrophoretic mobility of rotigotine·HCl ($1.49 \pm 0.04 \times 10^{-4}$ cm^2 s^{-1} V^{-1}) (*t*-test; $p = 0.134$).

3.2. Passive diffusion of rotigotine·H_3PO_4

A series of iontophoretic transport studies under various conditions were performed. During 6 h prior to iontophoresis, no current was applied and passive transport reached steady-state conditions within this period. From the slope of the linear part of the cumulative flux vs. time profile, the passive steady-state flux ($Flux_{pss}$) was calculated. Firstly, rotigotine·H_3PO_4 and rotigotine·HCl both at a concentration of 3.7 mM, buffered at pH 5, showed no significant difference in $Flux_{pss}$ (*t*-test; $p > 0.05$) (Table 2). Secondly, the results of transport studies of rotigotine·H_3PO_4 at various donor concentrations, comparing a donor pH of 5 and 6 are depicted in Fig. 1. A nonlinear hyperbolic fit showed a correlation between the $Flux_{pss}$ and the donor concentration at pH 5 ($R^2 = 0.889$). Increasing the pH

Table 1
The solubility of rotigotine·H_3PO_4 and rotigotine·HCl in different medium at pH 4, 5 and 6 in the presence and absence of 68 mM NaCl ($n = 2$–3).

pH	Rotigotine·H_3PO_4		Rotigotine·HCl*	
	No NaCl mM (mean)	68 mM NaCl mM (mean)	No NaCl mM (mean ± SD)	68 mM NaCl mM (mean ± SD)
4.00	83.48[a]	80.08[c]	24.39 ± 4.66 [a,b]	6.75 ± 0.31 [b,c]
5.00	41.89[a]	42.95[c]	22.45 ± 0.63 [a,b]	6.35 ± 0.34 [b,c]
6.00	15.67	14.44[d]	15.87 ± 1.25 [b]	6.52 ± 0.17 [b,d]

[a] $p < 0.001$.
[b] $p < 0.001$.
[c] $p < 0.001$.
[d] $p < 0.01$.
* The values were adapted from reference [3].

Table 2
Comparison of the iontophoretic flux of rotigotine·H_3PO_4 with rotigotine·HCl at pH 5 in the presence of 68 mM NaCl. Results are presented as mean ± SD (n = 3–4).

Donor phase compound	Results		
	Conc. (mM)	Passive $Flux_{ss}$ nmol cm^{-2} h^{-1} (mean ± SD)	Iontophoretic $Flux_{ss}$ nmol cm^{-2} h^{-1} (mean ± SD)
Rotigotine·HCl	3.77	1.7 ± 0.8	69.4 ± 6.4
Rotigotine·H_3PO_4	3.74	1.6 ± 0.4	73.8 ± 12.6

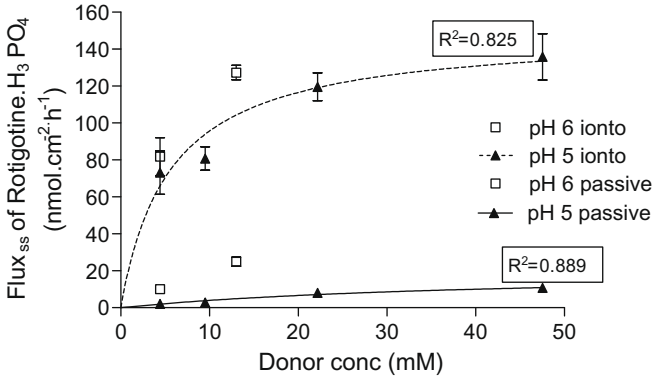

Fig. 1. The $Flux_{ss}$ of rotigotine·H_3PO_4 during the passive phase (no current) and the iontophoretic phase (current density = 500 μA cm^{-2}) at various donor concentrations at donor pH 5 (closed triangle) and pH 6 (open square). The correlation of the $Flux_{ss}$ vs. donor concentration was determined at pH 5. The line of correlation of the passive $Flux_{ss}$ vs. donor concentration is full, and the line of correlation of the iontophoretic $Flux_{ss}$ vs. donor concentration is intermittent. Data are presented as mean ± SD (n = 3).

of the donor phase from 5 to 6 increased the passive flux of rotigotine·H_3PO_4 quite drastically: close to saturation of rotogotine·H_3PO_4 in the donor phase the maximum flux that could be achieved was 10.8 ± 1.9 nmol cm^{-2} h^{-1} at pH 5 and 24.9 ± 2.5 nmol cm^{-2} h^{-1} at pH 6.

3.3. Iontophoresis of rotigotine·H_3PO_4

A series of iontophoretic transport studies was conducted to investigate the iontophoretic transport of rotigotine·H_3PO_4 specially focusing on: (i) comparison with the iontophoretic flux of rotigotine·HCl, (ii) the relationship between the flux and donor concentration, (iii) the influence of the pH, (iv) the contribution of the electro-osmotic flow and (v) the determination of the transport number.

3.3.1. Flux of rotigotine·H_3PO_4 vs. rotigotine·HCl

During the transport studies after 6 h of passive diffusion, a current density was applied of 500 μA cm^{-2} during 9 h. The steady-state flux ($Flux_{ss}$) of rotigotine·H_3PO_4 during iontophoresis showed no significant difference to the $Flux_{ss}$ of rotigotine·HCl ($p > 0.05$) (Table 2).

3.3.2. $Flux_{ss}$ as function of donor concentration rotigotine·H_3PO_4 and influence of pH in donor formulation

As shown in Fig. 2, current application resulted in an immediate increase in the flux of rotigotine·H_3PO_4, which reached steady-state within 4 h. The results of a series of iontophoretic transport studies of rotigotine·H_3PO_4 at pH 5 and pH 6 are depicted in Fig. 1. A nonlinear relationship could be described between the $Flux_{ss}$ and the donor concentration at pH 5 (R^2 = 0.825). Thereby, the $Flux_{ss}$ at equal rotigotine·H_3PO_4 concentration increased with

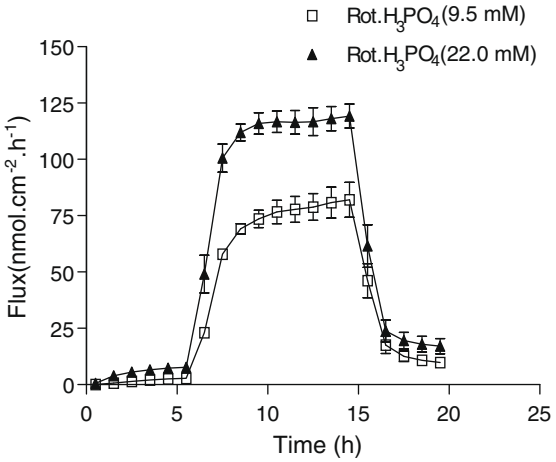

Fig. 2. The iontophoretic flux vs. time profile of rotigotine·H_3PO_4 dissolved in citric buffer pH 5 at two different concentrations, 9.5 mM (open square) and 22.0 mM (closed triangle). Data are presented as mean ± SD (n = 3).

increasing pH of the donor solution. However, close to saturation in the donor phase, the $Flux_{ss}$ at pH 5 (135.8 ± 12.5 nmol cm^{-2} h^{-1}) was not significantly different from the Flux at pH 6 (127.3 ± 4.0 nmol cm^{-2} h^{-1}) (t-test; $p > 0.05$).

3.3.3. Electro-osmotic contribution

To quantify the electro-osmotic contribution, acetaminophen was co-transported with rotigotine. The electro-osmotic flux was investigated at two different concentrations rotigotine·H_3PO_4 (3.9 and 11.6 mM) at pH 5 in the donor phase. The relative contributions of J_{pass}, J_{EO} and J_{EM} are depicted in Fig. 3. With increasing donor concentrations, the relative contribution of the passive flux significantly increased from 13.1 ± 0.1% for 3.9 mM to 17.6 ± 0.1% for 11.6 mM (t-test; $p < 0.05$). An increase in rotigotine·H_3PO_4 concentration from 3.9 mM to 11.6 mM resulted in a significant decrease in the relative contribution of the electro-osmotic flow from 5.1 ± 0.1% to 2.8 ± 0.3% (t-test; $p < 0.05$). Electromigration was the main driving force and accounted for 81.8 ± 0.03 and 79.5 ± 0.1% of the total flux of 3.9 mM and 11.6 mM rotigotine·H_3PO_4, respectively.

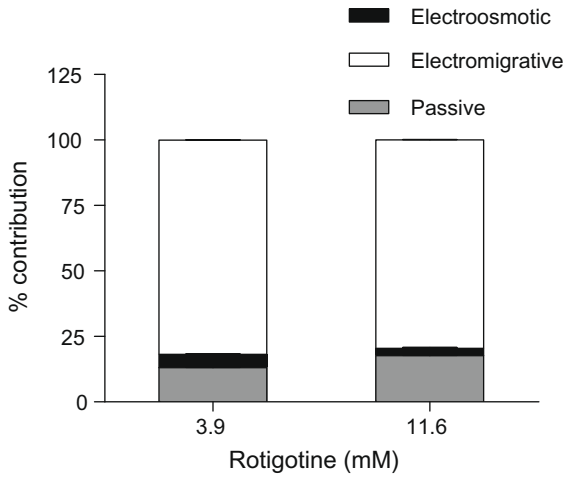

Fig. 3. The relative contribution of the passive (grey), electro-osmotic (black) and electromigrative (white) flux to the total (100%) flux of rotigotine·H_3PO_4 at two different concentrations (3.9 and 11.6 mM). The donor phase was buffered at pH 5, and the applied current density was 500 μA cm^{-2}. Data are presented as mean ± SD (n = 3).

Table 3
Best-fit results of the estimated parameters, steady-state flux ($Flux_{ss}$) release constant (K_R), the lag time (t_L) and the passive flux post-iontophoresis (pass) and comparison to the value obtained with the permeation lag-time method. The data are presented as mean and standard error of the mean (SEM). Furthermore, values of the elimination constant (k_e), clearance (Cl) and apparent volume of distribution, considering the bioavailability (Vd/F) of rotigotine as found in the literature, are depicted.

	Unit	Model prediction		Permeation lag-time method		Literature values*
		Best-fit value	SEM	Best-fit value	SEM	
$Flux_{ss}$	nmol cm^{-2} h^{-1}	135	3.56	135.8	4.18	
K_R	h^{-1}	1.08	0.04	n.d.		
t_L	h^{-1}	Negligible		n.d.		
Pass	h	12.3	0.4	n.d.		
k_e	h^{-1}					0.125
Cl	l h^{-1}					450
Vd/F	l					3600

n.d.: Not determined.
* Values were adapted from references [15–20].

3.3.4. Determination of transport number

With increasing pH from 5 to 6, a decrease in solubility, but an increase in delivery efficiency was observed. At pH 5.5 a balance is expected between maximum solubility and delivery efficiency. At this selected pH, under near to saturated conditions, the transport number was determined. Therefore, in a single experiment the relationship between the $Flux_{ss}$ and the current density was studied with a donor phase containing 31.3 mM rotigotine·H_3PO_4, which was 90% of the maximum solubility of rotigotine·H_3PO_4. An increase in the current density resulted in a significant increase in flux, which reached steady-state within 6 h of current application. A current density of 0 μA cm^{-2} (passive phase), 166 μA cm^{-2}, 333 μA cm^{-2} and 500 μA cm^{-2} resulted in a $Flux_{ss}$ of 24.4 ± 1.9 nmol cm^{-2} h^{-1}, 65.8 ± 9.3 nmol cm^{-2} h^{-1}, 109.7 ± 15.7 nmol cm^{-2} h^{-1} and 154.5 ± 27.0 nmol cm^{-2} h^{-1}, respectively. An excellent linear correlation could be observed between the $Flux_{ss}$ and the current density (R^2 = 0.999). The transport number was calculated from the slope of the correlation at 0.7%.

3.4. Modeling in vitro iontophoretic transport of rotigotine·H_3PO_4

The *in vitro* iontophoretic transport across HSC was analyzed using compartment modeling. The kinetic model to describe the flux was based on zero-order mass transport from donor to skin and a first-order release from skin to acceptor. The best-fit results and the standard error of the mean (SEM) of $Flux_{ss}$, the first-order release constant (K_R), the lag time (t_L) and the passive flux post-iontophoresis (pass) can be found in Table 3. No significant difference could be observed between the best fit of $Flux_{ss}$, estimated by the compartmental model and by the permeation lag-time method (*t*-test; $p > 0.05$).

The quality of fitting and model parameter estimation was evaluated graphically. The diagnostic plots of the model can be found in Fig. 4. The population predicted (PRED) vs. the observed flux (Fig. 4, panel A) and the individual predicted (IPRED) vs. the observed flux (Fig. 4, panel B) show that the model can describe adequately the *in vitro* iontophoretic transport. Moreover, the visual predictive check, displayed in Fig. 4, panel C, demonstrates that the observed data are well distributed in the 95% confidence interval of the simulated data. This suggests that the variability, predicted by the model, represents the variability of the actual observed data.

4. Discussion

4.1. Solubility

In a previous study, one of the major limitations in the iontophoretic transport of rotigotine·HCl was its low solubility. The maximum solubility of rotigotine·HCl was only 7.1 ± 0.4 mM at pH 5. In that study, the iontophoretic transport at varying rotigotine·HCl concentrations between 1.4 and 3.9 mM showed a linear relationship between the $Flux_{ss}$ and the donor concentration [2]. This demonstrated that the maximum iontophoretic flux of rotigotine was not yet achieved, but the low solubility of rotigotine·HCl was the limiting factor for further increase in the iontophoretic flux. Higher donor concentrations could be achieved by replacing HCl by another salt [11,12]. As shown in Table 1, in the presence of 68 mM NaCl, the solubility of rotigotine increased substantially when HCl was replaced by H_3PO_4. Compared to rotigotine·HCl, the solubility of rotigotine·H_3PO_4 is 2-, 6-, 10-fold higher at pH 6, 5 and 4, respectively. Furthermore, in contrast to the solubility of the HCl salt, the presence of NaCl did not affect the solubility of rotigotine·H_3PO_4. This can be explained by an absence of the common-ion effect. The next step was to investigate the transdermal delivery of rotigotine as H_3PO_4 salt.

4.2. In vitro transdermal delivery

The transdermal passive delivery of rotigotine·H_3PO_4 (3.77 mM) was investigated in comparison with rotigotine·HCl at the same donor concentration (3.74 mM). At pH 5, no difference in passive delivery could be observed. The solubility of rotigotine·HCl at pH 5 was lower compared to the solubility of rotigotine·H_3PO_4. The higher thermodynamic activity of rotigotine·HCl under these conditions was expected to result in a higher passive flux for rotigotine·HCl [13]. It seems that replacement of HCl by H_3PO_4 in the rotigotine salt not only increases the solubility of rotigotine, but also increases the efficiency in passive transport of rotigotine across HSC. In analogy to the passive flux, no difference in total iontophoretic flux could be observed between rotigotine·H_3PO_4 (3.77 mM) and rotigotine·HCl (3.74 mM). This observation is strengthened by the observed equal electrophoretic mobility of both salt forms, determined with capillary electrophoresis. This indicates that under these conditions, an equal part of the current is carried by rotigotine, regardless of its salt form, resulting in the same total iontophoretic flux.

The use of rotigotine·H_3PO_4 compared to that of rotigotine·HCl has two major advantages: (i) Increasing the donor pH from 5 to 6 significantly increases the passive flux of rotigotine·H_3PO_4. The maximum solubility of rotigotine·H_3PO_4 at pH 6 is much lower than at pH 5. Consecutively, the thermodynamic activity at equal concentration of this compound is higher at pH 6, which results in an increased passive diffusion [14]. Due to this increase in passive flux, an increase in total flux during the iontophoresis period was also observed with increasing pH. In contrast, the total iontophoretic flux of rotigotine·HCl did not change when the pH was increased from 5 to 6 [3]. (ii) The second advantage is the increase in maximum solubility of rotigotine·H_3PO_4 compared to that of rotigotine·HCl. Due to a higher

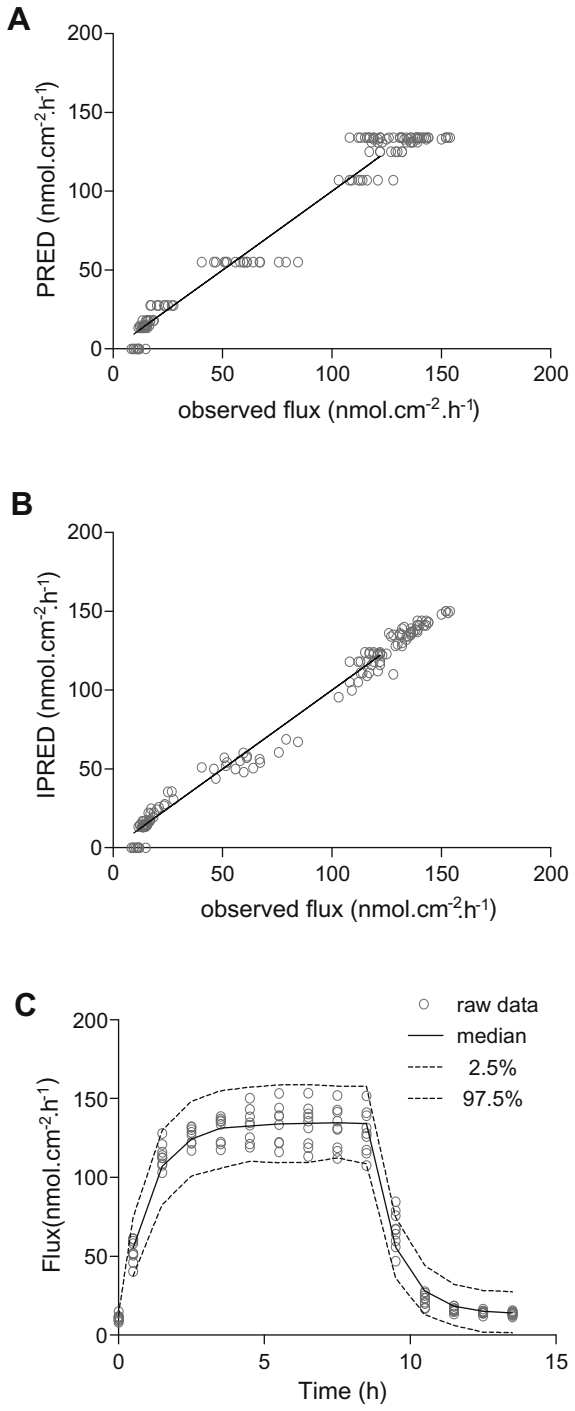

Fig. 4. Diagnostic plots of the compartmental modeling of the *in vitro* iontophoretic transport of rotigotine (47 mM), buffered at pH 5. Panel A: plot of the population-predicted flux (PRED) vs. the observed flux. Panel B: plot of the individual-predicted flux (IPRED) vs. the observed flux. Panel C: visual predictive check of the *in vitro* model: raw data superimposed on median, 2.5th and 97.5th percentiles of data simulated from model. Median (full line); 2.5th and 97.5th percentile (dashed line; raw data (open circle).

maximum solubility of the phosphate salt, higher donor concentrations of rotigotine can be obtained. Iontophoretic delivery of higher donor concentrations results in an increase in the maximum iontophoretic transport. At pH 5, the maximum iontophoretic flux of rotigotine·HCl was 80.2 ± 14.4 nmol cm^{-2} h^{-1}, while with rotigotine·H_3PO_4 a maximum flux of 135.8 ± 12.5 nmol cm^{-2} h^{-1} was achieved [2]. This means that the maximum flux can be increased with 170% by replacing the HCl salt with a H_3PO_4 salt. Besides a higher flux, another practical advantage can be established when using a high donor concentration at pH 5. Calculations revealed that after 24 h, maintaining a maximum flux of 135.8 nmol cm^{-2} h^{-1}, the amount rotigotine·H_3PO_4 in the donor phase decreased with 35%. This decrease in donor concentration would result only in a decrease of 10% in steady-state flux. This shows that with a high donor concentration, a high flux can be maintained for a long time. Taking these results together, one must seek a balance between transport efficiency and donor concentration by choosing the pH of the donor solution. On the one hand, by increasing the pH, it is possible to increase the transport efficiency; however, the limited solubility of the compound at pH 6 prevents the use of a high concentration. On the other hand, at pH 5, the transport efficiency is lower; nonetheless, a high flux can be established for a long time due to the higher solubility of rotigotine·H_3PO_4.

The total flux is driven by the passive, electromigrative and electro-osmotic flux. The electro-osmotic contribution of rotigotine·H_3PO_4, estimated at 5%, is higher than the electro-osmotic contribution of rotigotine·HCl, calculated at 2.3% [2]. This is mainly due to the higher concentration of rotigotine·H_3PO_4 in the donor formulation. Nonetheless, the main driving force of the iontophoretic delivery of both salt forms remains electromigration and in case of rotigotine·H_3PO_4 accounts for approximately 80% of the total flux at two different concentrations (Fig. 3). The transport number of rotigotine·H_3PO_4 at pH 5.5 was estimated from the slope of relationship between the $Flux_{ss}$ and the current density at 0.7%. This is higher than the transport number of rotigotine·HCl (0.4%) at pH 5, which can be explained by a higher donor concentration of rotigotine·H_3PO_4 [2].

4.3. From in vitro modeling to in vivo simulation

After characterizing and optimizing the transdermal delivery of this promising compound *in vitro*, the potential of the iontophoretic delivery of rotigotine *in vivo* was evaluated. A series of simulations were performed, using pharmacokinetic modeling. The first step was to determine the parameters driving the iontophoretic delivery *in vitro* across human stratum corneum of rotigotine·H_3PO_4 (47 mM), buffered at pH 5. The value of the $Flux_{ss}$ corresponds well with the value estimated by the permeation lag-time method (Table 3). In addition, diagnostic plots of the data modeling (Fig. 4) confirm that this model successfully describes the *in vitro* iontophoretic transport of rotigotine·H_3PO_4. In the next step, the apparent pharmacokinetic parameters of rotigotine, reported in the literature, are combined with the best-fit values of $Flux_{ss}$, K_R and t_L to predict the plasma levels *in vivo* [15–20]. A comparison was made with the passive delivery of rotigotine. Neupro, a passive transdermal delivery system of rotigotine, is approved by the EMEA for symptomatic treatment of Parkinson's disease [21]. The patch delivers 1–8 mg rotigotine in 24 h, depending on the patch size. As reported in the literature, passive delivery of rotigotine with a patch size of 10 cm^2, estimated to deliver 2 mg in 24 h, resulted in a maximum plasma concentration (C_{max}) of 215 pg ml^{-1} at 16 h [22]. Two different protocols were used to evaluate the iontophoretic delivery of rotigotine (47 mM, pH 5) during 24 h. As shown in Fig. 5, applying a current density of 350 μA cm^{-2} during 24 h (protocol 1) is expected to result in C_{max} of 630 pg ml^{-1}. Not only can a higher flux be established with iontophoresis, but more interestingly already at time = 5 h a plasma concentration of 240 pg ml^{-1} can be reached. Therefore, the *in vivo* iontophoretic delivery of rotigotine was simulated using protocol 2, applying initially a current density of 350 μA cm^{-2} for 5 h, after which the current density was decreased to 150 μA cm^{-2}. These simulations demonstrate two very important advantages of iontophoretic delivery of rotigotine in combination with iontophoresis over transdermal passive diffusion. Firstly, because

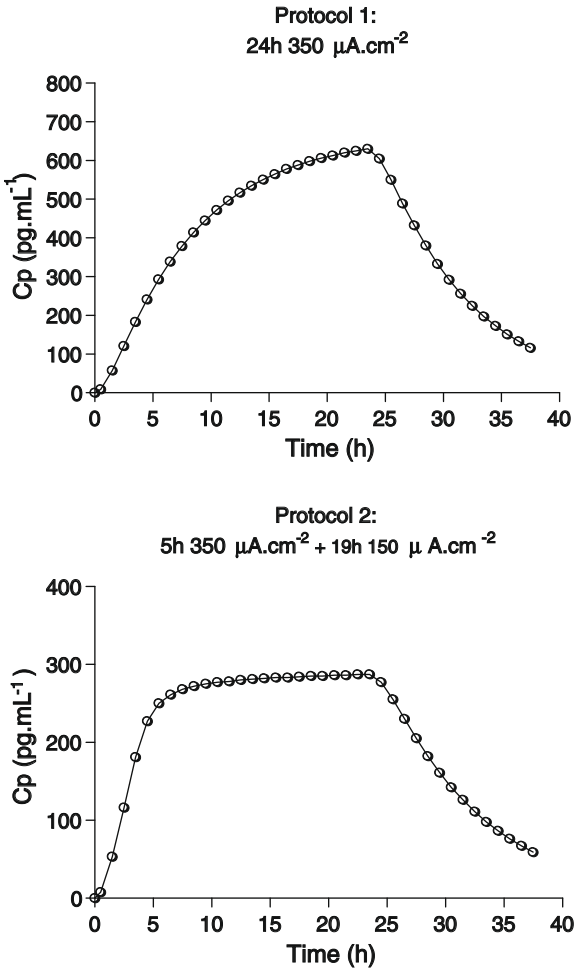

Fig. 5. Population prediction of the simulations of iontophoretic delivery of rotigotine·H_3PO_4 (47 mM) using different protocols: Protocol 1: 24 h 350 µA cm^{-2}; Protocol 2: 5 h 350 µA cm^{-2} + 19 h 150 µA cm^{-2}. The open circles are the population prediction of the simulated plasma concentration (Cp).

of active transdermal delivery, the onset time to achieve the desired level can be significantly decreased. Secondly, by adjusting the current density, a titration of the plasma concentration is possible, making it feasible to individually modulate the delivery according to the desired dosing regimen. Both advantages can be of great benefit for symptomatic treatment of Parkinson's disease.

In conclusion, despite the lipophilicity of rotigotine, high levels can be achieved with transdermal iontophoretic delivery with a rapid onset time, making it a very promising compound for symptomatic treatment of Parkinson's disease. Thereby, changing the salt form of a drug can improve the physicochemical properties and consequently the maximal transdermal transport of a therapeutic drug, without changing its major transport mechanisms.

Acknowledgments

This work was supported by UCB Schwarz Biosciences GmbH, Monheim, Germany. The authors would also like to thank Willi Cawello (UCB Schwarz Biosciences GmbH, Monheim, Germany) for providing the correct pharmacokinetic data concerning the transdermal delivery of rotigotine.

References

[1] P.L. Honeywell-Nguyen, S. Arenja, J.A. Bouwstra, Skin penetration and mechanisms of action in the delivery of the D2-agonist rotigotine from surfactant-based elastic vesicle formulations, Pharmaceutical Research 20 (10) (2003) 1619–1625.
[2] A.K. Nugroho, G. Li, A. Grossklaus, M. Danhof, J.A. Bouwstra, Transdermal iontophoresis of rotigotine: influence of concentration, temperature and current density in human skin in vitro, J Control Release 96 (1) (2004) 159–167.
[3] A.K. Nugroho, G.L. Li, M. Danhof, J.A. Bouwstra, Transdermal iontophoresis of rotigotine across human stratum corneum in vitro: influence of pH and NaCl concentration, Pharmaceutical Research 21 (5) (2004) 844–850.
[4] A.T. Serajuddin, Salt formation to improve drug solubility, Advanced Drug Delivery Reviews 59 (7) (2007) 603–616.
[5] J. Fang, R. Wang, Y. Huang, P.C. Wu, Y. Tsai, Passive and iontophoretic delivery of three diclofenac salts across various skin types, Biological and Pharmaceutical Bulletin 23 (11) (2000) 1357–1362.
[6] J.Y. Fang, R.J. Wang, Y.B. Huang, P.C. Wu, Y.H. Tsai, Influence of electrical and chemical factors on transdermal iontophoretic delivery of three diclofenac salts, Biological and Pharmaceutical Bulletin 24 (4) (2001) 390–394.
[7] O. Ackaert, J. De Graan, R. Capancioni, D. Dijkstra, M. Danhof, J.A. Bouwstra, Transdermal iontophoretic delivery of a novel series of dopamine agonists in vitro: physicochemical considerations, submitted for publication.
[8] A.K. Nugroho, L. Li, D. Dijkstra, H. Wikstrom, M. Danhof, J.A. Bouwstra, Transdermal iontophoresis of the dopamine agonist 5-OH-DPAT in human skin in vitro, J Control Release 103 (2) (2005) 393–403.
[9] A.K. Nugroho, S.G. Romeijn, R. Zwier, J.B. de Vries, D. Dijkstra, H. Wikstrom, O. Della-Pasqua, M. Danhof, J.A. Bouwstra, Pharmacokinetics and pharmacodynamics analysis of transdermal iontophoresis of 5-OH-DPAT in rats: in vitro–in vivo correlation, Journal of Pharmaceutical Sciences 95 (7) (2006) 1570–1585.
[10] N. Holford, The Visual Predictive Check-Superiority to Standard Diagnostic (Rorschach) Plots. PAGE 14, Abstr 738 <http://www.page-meeting.org/?abstract=738>, (2005).
[11] S.M. Berge, L.D. Bighley, D.C. Monkhouse, Pharmaceutical salts, Journal of Pharmaceutical Sciences 66 (1) (1977) 1–19.
[12] S. Li, S. Wong, S. Sethia, H. Almoazen, Y.M. Joshi, A.T. Serajuddin, Investigation of solubility and dissolution of a free base and two different salt forms as a function of pH, Pharmaceutical Research 22 (4) (2005) 628–635.
[13] T. Higuchi, Physical chemical analysis of percutaneous absorption process from creams and ointments, Journal of the Society of Cosmetic Chemists 11 (1960) 85–97.
[14] C.W. Jeans, C.M. Heard, A therapeutic dose of primaquine can be delivered across excised human skin from simple transdermal patches, International Journal of Pharmaceutics 189 (1) (1999) 1–6.
[15] L. Schwarz pharma, Neupro®, Mequon, WI, 2007.
[16] W. Cawello, M. Braun, R. Horstmann, T. Funaki, Y. Tadayasu, Pharmacokinetics, safety and tolerability of rotigotine after transdermal patch administration in Japanese and Caucasian healthy subjects, Movement Disorders 21 (S15) (2006) S547.
[17] W. Cawello, M. Braun, H. Boekens, (A) DME of the dopamine agonist rotigotine in man, Drug Metabolism and Disposition 37 (10) (2009) 2055–2060.
[18] W. Cawello, M. Braun, R. Horstmann, Pharmacokinetics of transdermal rotigotine in subjects with impaired renal function, in: ACCP 34th Annual Meeting, Rockville, MD, 2005.
[19] W. Cawello, J. Elshoff, H. Boekens, M. Braun, R. Horstmann, Characteristics of rotigotine elimination after patch removal, European Journal of Neurology 13 (suppl. 2) (2006) 85.
[20] W. Cawello, H.M. Wolff, W.J. Meuling, R. Horstmann, M. Braun, Transdermal administration of radiolabelled [14C] rotigotine by a patch formulation: a mass balance trial, Clinical Pharmacokinetics 46 (10) (2007) 851–857.
[21] EMEA. European Public Assessment Report (EPAR), Annex I: Summary of Product Characteristics for Neupro. <http://www.emea.europa.eu/humandocs/PDFs/EPAR/neupro/H-626-PI-en.pdf>, 2009.
[22] W. Cawello, R. Horstmann, Pharmacokinetics of transdermal rotigotine in subjects with impaired renal function, in: ACCP 34th Annual Meeting, Rockville, MD, 2005.